

COMPOSITIONAL ANALYSIS OF DRUGS BY LASER-INDUCED BREAKDOWN SPECTROSCOPY

S. A. Beldjilali,^{a,b*} E. Axente,^c A. Belasri,^b
T. Baba-Hamed,^b and J. Hermann^a

UDC 621.373.8;533.9;615.03

The feasibility of the compositional analysis of drugs by calibration-free laser-induced breakdown spectroscopy (LIBS) was investigated using multivitamin tablets as a sample material. The plasma was produced by a frequency-quadrupled Nd:YAG laser delivering UV pulses with a duration of 5 ns and an energy of 12 mJ, operated at a repetition rate of 10 Hz. The relative fractions of the elements composing the multivitamin drug were determined by comparing the emission spectrum of the laser-produced plume with the spectral radiance computed for a plasma in a local thermodynamic equilibrium. Fair agreement of the measured fractions with those given by the manufacturer was observed for all elements mentioned in the leaflet of the drug. Additional elements such as Ca, Na, Sr, Al, Li, K, and Si were detected and quantified. The present investigations demonstrate that laser-induced breakdown spectroscopy is a viable technique for the quality control of drugs.

Keywords: laser-induced breakdown spectroscopy, plasma modeling, calibration-free approach, quality control of drugs, multivitamin tablet.

Introduction. Drug safety has become a major concern in the pharmaceutical industry due to the globalization of the drug market. Indeed, the development of the black market and e-commerce of drugs can lead to the manufacturing of uncertified products in both developing and developed countries. Moreover, raw synthesis ingredients such as plants can be a source of contamination with toxic heavy metals such as arsenic, lead, cadmium, and mercury.

In order to have an accurate quantification of the concentrations of trace elements in drugs, new analytical methods have been developed in order to improve the sensitivity and measurement accuracy, preferably *in situ* and in real time. Nowadays, a broad range of analytical techniques such as titrimetric, chromatographic, spectroscopic, electrophoretic, and electrochemical, and their corresponding methods are currently applied in the analysis of pharmaceuticals [1].

Recently, laser-induced breakdown spectroscopy (LIBS) has been extended to the analysis of all kinds of materials and can be applied in different areas such as biology, forensic medicine, healthcare [2–6], metallurgy [7, 8], mining, and the pharmaceutical industry [9–11]. It was shown that LIBS can quantify many toxic elements at ppm levels such as aluminum (50 ppm) and strontium (1 ppm) embedded in an organic matrix [12]. In addition to the recent technological developments of the LIBS technique such as spectrometers, lasers, and optical systems, studies have reported on the development of simulation codes for modeling the plasma emission spectrum and for measuring the elemental concentrations of the sample.

The calibration-free LIBS approach used in this study was previously validated for the quantitative analyses of both organic [6, 12] and inorganic materials [7, 13–17]. It is based on the calculation of the spectral radiance of the plasma in local thermodynamic equilibrium (LTE). The model accounts for self-absorption and possible nonuniform spatial distributions of temperature and density [13]. A multivitamin tablet was used as a sample in order to evaluate the feasibility of calibration-free LIBS for the measurements of the elemental composition of drugs.

Experimental. The plasma was produced by a frequency-quadrupled Nd:YAG laser delivering UV pulses with a duration of 5 ns and an energy of 12 mJ, operated at a repetition rate of 10 Hz. The tablet was placed inside a vacuum chamber,

*To whom correspondence should be addressed.

^aLP3 CNRS – Aix-Marseille University, 13288 Marseille, France; ^bLPPMCA Université des Sciences et de la Technologie d'Oran Mohamed Boudiaf, USTO-MB, 31000 Oran, Algeria; e-mail: sidahmed.beldjilali@univ-usto.dz; ^cLSPI National Institute for Lasers, Plasma, and Radiation Physics, 077125 Măgurele-Bucharest, Romania. Published in Zhurnal Prikladnoi Spektroskopii, Vol. 84, No. 3, pp. 457–462, May–June, 2017. Original article submitted February 11, 2016.

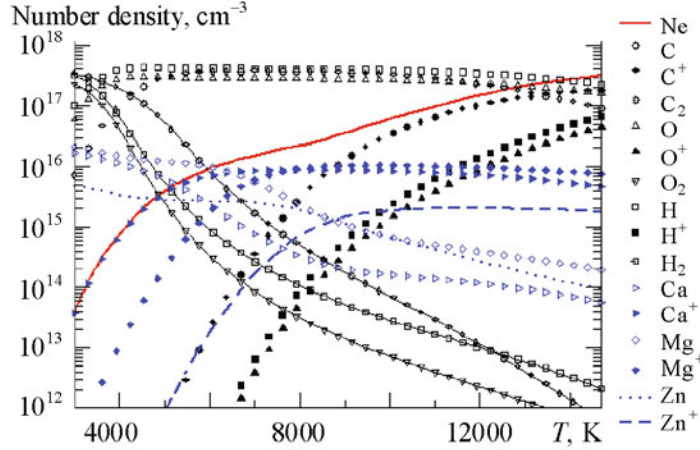


Fig. 1. Number densities of species (Mg, Zn, Ca, C, C₂, O, O₂, H, and H₂) versus plasma temperature, measured for a plasma of 1×10^5 Pa pressure.

the target irradiation being performed in air, using a laser fluence of about 60 J/cm^{-2} . For spectroscopic measurements, the photon emitted from the plume was detected using an Echelle spectrometer coupled with an ICCD camera. The spectral resolution of the spectrometer is $\lambda/\Delta\lambda \cong 9 \times 10^3$. To improve the signal-to-noise ratio, we applied 50 pulses on 30 irradiation sites. The entire experiment was conducted under the same synchronization conditions: the gate width was 5000 ns, and the gate delay was 1000 ns. More information and details on the experimental setup and the intensity calibration were published in our previous papers [6, 7, 12, 13].

Results and Discussion. The relative fractions of elements in the multivitamin tablet were determined by fitting the emission spectrum of the laser-produced plume to the spectral radiance of a plasma in the LTE condition [13]. Our simulation model takes into consideration self-absorption, which is of particular significance in the present case, where major elements are considered [14, 15]. The following requirements must be satisfied: (i) the plume is in LTE, (ii) the ablation process is stoichiometric, and (iii) there is no segregation in the plume. Furthermore, the measurement procedure may take into account the density and temperature gradients. This simplification was shown to give satisfactory results for the concentration measurements of metals when only atomic spectral lines were chosen for investigation [16, 17]. More information and details on the theoretical background of our calibration-free procedure were reported in [6, 7, 12, 13].

The determination of the plasma temperature T and the electron density n_e helps to measure the plasma composition. The number density of plasma species computed for a multivitamin tablet of typical elemental composition is represented as a function of temperature in Fig. 1. The calculation was performed by setting the pressure to a constant value equal to the pressure of ambient air. The plasma is dominated by neutral atoms for $T < 6000$ K, whereas ions dominate at higher temperatures. The electron density equals the density of calcium for $T < 6000$ K, whereas the contribution of calcium ionization becomes significant at higher temperatures. For $T < 8000$ K, the electrons in the plasma are generated from metals. On the other hand, for higher temperatures, the electrons are due to the ionization of organic atoms.

The electron temperature profiles were obtained assuming the presence of LTE. Essentially this assumption states that for each registered emission spectrum the electrons in the plasma are in a state of thermal equilibrium. The electron velocities are represented by the Maxwell distribution and the electron temperature T_e . Additionally, the Boltzmann distribution provides a valid description of the excited states population with the same temperature parameter T_e . The fact that the values of these two temperatures converge has an important consequence for the physical nature of the optical excitation. It indicates, in particular, that the overwhelming part of the atomic excitation was caused by collisions and not by radiation. Assuming the presence of LTE assumption and considering atoms of the same species, the intensity ratio I_1/I_2 of the two-emission lines λ_1 and λ_2 can be calculated by

$$I_1/I_2 = (\lambda_2/\lambda_1)(g_1A_1/g_2A_2) \exp [(E_2 - E_1)/k_B T_e], \quad (1)$$

where g_1 and g_2 indicate a degeneration of upper states of the considered emission lines λ_1, λ_2 , and A_1, A_2 their corresponding transition probabilities given by Einstein's coefficients.

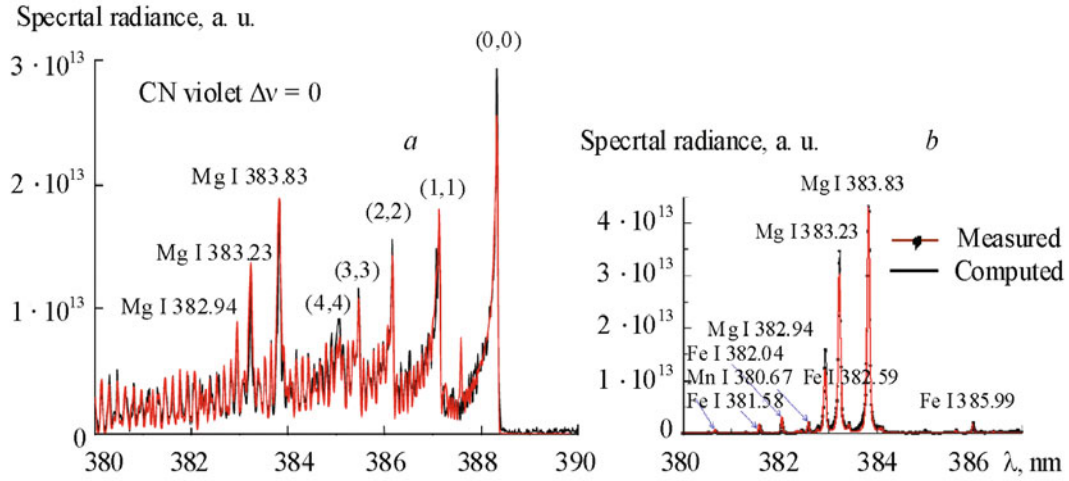


Fig. 2. Experimental and simulated spectra for laser ablation of multivitamin tablet of a multiplet of magnesium $^3P^0-^3D$ recorded at 1000 ns gate delay and 500 ns gate width (a); and 1000 ns gate delay and 5000 ns gate width (b). CN molecular emission is detected in (a).

TABLE 1. Transition Probability A_{ul} , Degeneration g , and Energy E of Lower and Upper Excitation Levels and Stark Width w and Shift d for $n_e = 1 \times 10^{17} \text{ cm}^{-3}$ of the Selected Transitions

Transition	A_{ul}, s^{-1}	E_l, cm^{-1}	g_l	E_u, cm^{-1}	g_u	w, pm	d, pm
Mg I 383.83	1.594×10^8 [18]	21911	5	47957	7	110 [32]	-2 [32]
Mg I 516.73	1.130×10^7 [19]	21850	1	41197	3	33 [32]	9 [32]
Mg I 518.36	5.464×10^7 [18]	21911	5	41197	3	35 [32]	7.4 [32]
Ca I 431.87	7.380×10^7 [20]	15316	5	38465	3	16 [33]	-
Fe I 252.28	2.923×10^8 [21]	0	9	39626	9	-	-
Fe II 252.54	1.828×10^8 [22]	21252	14	60838	14	-	-
Fe I 358.12	1.018×10^8 [21]	6928	11	34844	13	-	-
Fe I 381.30	7.910×10^6 [23]	7728	7	33947	5	-	-
Na I 588.99	6.289×10^7 [20]	0	2	16973	4	75 [34]	11 [34]
Mn I 403.08	1.738×10^7 [24]	0	6	24802	8	57 [32]	-
Mn I 407.92	1.523×10^7 [25]	17282	8	41789	10	-	-
Sr II 407.77	1.472×10^8 [26]	0	2	24517	4	-	-
Sr I 460.73	2.817×10^7 [27]	0	1	21698	3	-	-
Zn I 481.05	7.004×10^7 [28]	32890	5	53672	3	(50)	(36)
Al I 396.15	1.010×10^8 [29]	112	4	25348	2	-	-
Cr I 357.87	1.483×10^8 [24]	0	7	27935	9	-	-
Si I 251.61	1.680×10^8 [30]	223	5	39955	5	-	-
Li I 670.78	3.721×10^7 [20]	0	2	14904	4	-	-
K I 769.90	3.802×10^7 [20]	0	2	12985	2	(400)	-
Mo I 379.83	6.894×10^7 [31]	0	7	26320	9	-	-

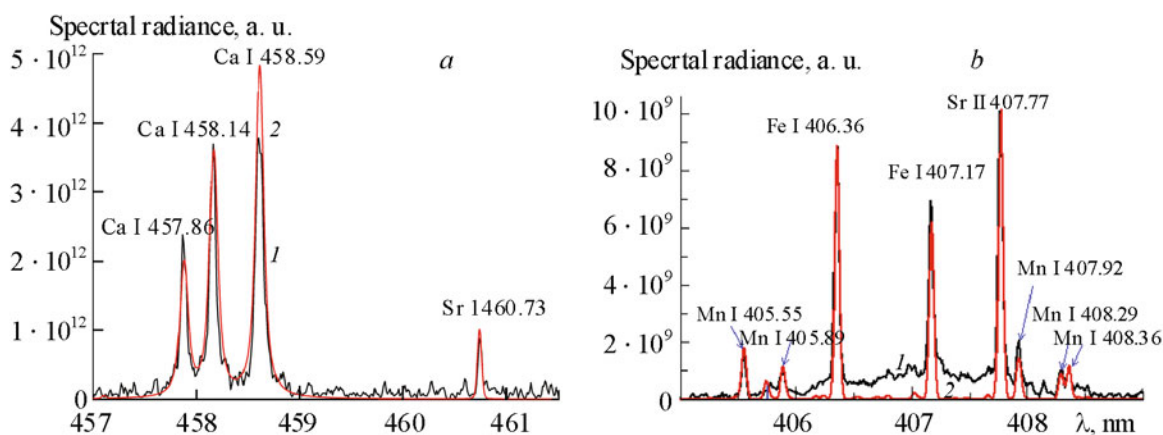


Fig. 3. Experimental (1) and simulated (2) spectra for laser ablation of multivitamin tablet recorded at 1000 ns gate delay and 5000 ns gate width and showing calcium and atomic strontium (a); and manganese, iron, and ionic strontium (b).

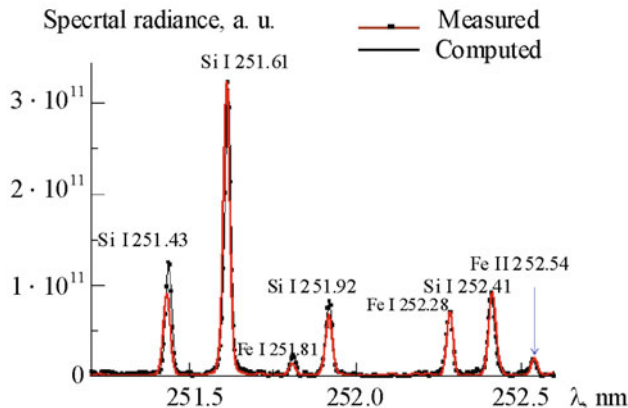


Fig. 4. Experimental and simulated spectra for laser ablation of multivitamin tablet of silicon and iron recorded at 1000 ns gate delay and 5000 ns gate width.

The multiplets $^3P^0-^3S$ and $^3P^0-^3D$ of magnesium atoms (Fig. 2b) have been used to evaluate the plasma temperature (Table 1), which was found to be around $T = 6700$ K. The measurement error, which depends on the gap between the two upper level energies, was about 10%. Experimental and simulated spectra were well matched for all selected spectral lines. It is important to optimize different LIBS parameters such as the delay time. As can be seen in Fig. 2, the violet molecular vibrational bands CN are observed just at a delay of 1000 ns and a gate width of 500 ns.

Magnesium was chosen as a reference element for our concentration measurements. Calculation started by giving an arbitrary value to this element. All concentrations of metallic elements that generated electrons in the plume were determined. The relative mass fractions of calcium, zinc, and potassium that have relative large concentrations in the multivitamin tablet were adjusted. The same procedure was applied to calculate the mass fractions of the remaining metals. Iron and chromium were identified by observing the Fe I 356.54, Fe I 357.01, and Fe I 358.12 nm atomic lines, and the Cr I 357.87 nm atomic line, respectively. Strontium was identified by observing the neutral Sr I 460.73 nm and Sr II 407.77 nm ionic lines (Fig. 3). The aluminum atomic resonance lines Al I 394.40 and Al I 396.15 nm were also detected although they were disrupted by the nearness of the two intense ionic lines of Ca II 393.37 and Ca II 396.85 nm. Manganese, molybdenum, and lithium lines were also identified. For the UV range, silicon lines were identified in Fig. 4, and the doublet of sodium Na I 589.00 and Na I 589.59 nm was also observed.

As stated before, only the relative mass fractions of metals were measured in this study. We chose magnesium as a reference due to its high concentration (4.5 wt.%). We assumed that the concentration given by the manufacturer for this

TABLE 2. Mass Fractions of Trace Elements Present in the Multivitamin Tablet

Element	Concentration for 1 tablet given in the leaflet of the drug, ppm	Concentration for 1 tablet measured by LIBS, ppm	Element	Concentration for 1 tablet given in the leaflet of the drug, ppm	Concentration for 1 tablet measured by LIBS, ppm	Element	Concentration for 1 tablet given in the leaflet of the drug, ppm	Concentration for 1 tablet measured by LIBS, ppm
I	100	–	Cr	25	30	Sr	–	70
Fe	5000	3900	Mn	400	840	Al	–	5
Zn	5000	9000	Mo	25	52	Li	–	7
Mg	45000 *	45000	Ca	–	64200	K	–	10000
Se	30	–	Na	–	2100	Si	–	2400

multivitamin tablet (weight of 1000 mg) was valid. The measured concentrations are shown in Table 2. A fair agreement is observed between the measured fractions and the values given by the manufacturer for all elements mentioned on the leaflet. Additional elements such as Ca, Na, Sr, Al, Li, K, and Si were detected, and their measured mass fractions vary from a few ppm to a few percent.

This study demonstrates that LIBS is a powerful analytical tool for concentration analysis without preliminary sample preparation. Our results are a confirmation of the high sensitivity of this method, which can be further developed and implemented for on-line drug processing monitoring and quality control.

Conclusions. A calibration-free LIBS approach was used to assess the relative elemental concentrations in a multivitamin tablet with a complex composition. Therefore, the plasma emission spectrum recorded during ultraviolet laser ablation was compared to the spectral radiance computed for a plasma in local thermodynamic equilibrium. Fair agreement was found between measured mass fractions and the composition given by the pharmaceutical manufacturer. Thirteen inorganic elements (Ca, Mg, K, Fe, Zn, Cr, Mn, Mo, Na, Sr, Al, Li, and Si) were detected in the present LIBS analysis and only eight elements were mentioned in the leaflet of the drug. This mismatch proves the need for complementary compositional analysis and an accurate estimation of measurement uncertainties.

REFERENCES

1. S. Görög, *Trend. Anal. Chem.*, **26**, No. 1 (2007)
2. E. M. Emara, H. Imam, M. A. Hassan, and S. H. Elnaby, *Talanta*, **117**, 176–183 (2013).
3. A.W. Miziolek, V. Palleschi, and I. Schechter, *Laser-Induced Breakdown Spectroscopy (LIBS) Fundamentals and Applications*, Cambridge University Press, Cambridge (2006).
4. V. Juvé, R. Portelli, M. Boueri, M. Baudelet, and J. Yu, *Spectrochim. Acta B*, **63**, 1047–1053 (2008).
5. W. Lei, V. Motto-Ros, M. Boueri, Q. Ma, D. Zhang, L. Zheng, H. Zeng, and J. Yu, *Spectrochim. Acta B*, **64**, 891–898 (2009).
6. S. Beldjilali, D. Borivent, L. Mercadier, E. Mothe, G. Clair, and J. Hermann, *Spectrochim. Acta B*, **65**, 727–733 (2010).
7. J. Hermann, A. Lorusso, A. Perrone, F. Strafella, C. Dutouquet, and B. Torralba, *Phys. Rev. E*, **92**, 053103(1–15) (2015).
8. M. Achouri, T. Baba-Hamed, S. A. Beldjilali, and A. Belasri, *Plasma Phys. Rep.*, **41**, No. 9, 758–768 (2015).
9. L. St-Onge, E. Kwong, M. Sabsabi, and E. B. Vadas, *Spectrochim. Acta B*, **57**, 1131–1140 (2002).
10. M. D. Mowery, R. Sing, J. Kirsch, A. Razaghi, S. Béchar, and R. A. Reed, *J. Pharm. Biomed. Anal.*, **28**, 935–943 (2002).
11. A. Nikolaou, S. Meric, and F. Despo, *Anal. Bioanal. Chem.*, **387**, 1225–1234 (2007).
12. S. A. Beldjilali, W. L. Yip, J. Hermann, T. Baba-Hamed, and A. Belasri, *Anal. Bioanal. Chem.*, **400**, 2173–2183 (2011).
13. E. Axente, J. Hermann, G. Socol, L. Mercadier, S. A. Beldjilali, M. Cirisan, C. Luculescu, C. Ristoscu, I. Mihailescu, and V. Craciun, *J. Anal. At. Spectrom.*, **29**, No. 3, 553–564 (2014).
14. J. Hermann, C. Gerhard, and E. Axente, C. Dutouquet, *Spectrochim. Acta B*, **100**, 189–196 (2014).
15. C. Gerhard, J. Hermann, L. Mercadier, L. Loewenthal, E. Axente, C. R. Luculescu, T. Sarnet, M. Sentis, and W. Viöl, *Spectrochim. Acta B*, **101**, 32–45 (2014).

16. J. Hermann, L. Mercadier, E. Mothe, G. Socol, and P. Alloncle, *Spectrochim. Acta B*, **65**, 636–641 (2010).
17. M. Boudhib, J. Hermann, and C. Dutouquet, *Anal. Chem.*, **88**, No. 7, 4029–4035 (2016).
18. E. M. Anderson, V. A. Zilitis, and E. S. Sorokina, *Opt. Spectr.*, **23**, 102 (1967).
19. R. L. Kurucz and E. Peytremann, *A Table of Semiempirical gf Values, SAO Special Report*, **362** (1975).
20. W. L. Wiese, M. W. Smith, and B. M. Miles, Atomic Transition Probabilities, **II**, U.S. Government Printing Office, Washington, DC, NSRDS-NBS **22** (1969).
21. J. R. Fuhr, G. A. Martin, and W. L. Wiese, *J. Phys. Chem. Ref. Data*, **17**, Suppl. 4 (1988).
22. R. L. Kurucz, *Trans. IAU*, **XXB**, Ed. M. McNally, Kluwer, Dordrecht, 168–172 (1988)
23. D. E. Blackwell, P. A. Ibbetson, A. D. Petford, and M. J. Shallis, *Mon. Not. Roy. Astron. Soc.*, **186**, 633 (1979).
24. G. A. Martin, J. R. Fuhr, and W. L. Wiese, *J. Phys. Chem. Ref. Data*, **17**, Suppl. 3 (1988).
25. D. E. Blackwell and B. S. Collins, *MNRAS*, **157**, 255 (1972).
26. B. Warner, *Mon. Not. Roy. Astron. Soc.*, **139**, 115–128 (1968)
27. C. H. Corliss and W. R. Bozman, *NBS Monogr.*, **53** (1962).
28. B. Warner, *Mon. Not. Roy. Astron. Soc.*, **140**, 53–59 (1968).
29. W. H. Smith and H. S. Liszt, *J. Opt. Soc. Am.*, **61**, 938 (1971).
30. L. J. Radziemski Jr. and K. L. Andrew, *J. Opt. Soc. Am.*, **55**, 474–491 (1965).
31. W. Whaling and J. W. Brault, *Phys. Scr.*, **38**, 707–718 (1988).
32. A. Lesage, *New Astron. Rev.*, **52**, 471–535 (2009).
33. N. Konjević and J. R. Roberts, *J. Phys. Chem. Ref. Data*, **5**, 209–257 (1976).
34. S. Bukvić, S. Djeniže, and A. Srećković, *Publ. Observ. Astron. Belgrade*, No. 50, 35–38 (1995).